Autonomous Non-Destructive Testing Robot

CSUN American Society of Mechanical Engineering

Team Members:

President**:** Ricky Chi Yam

Project Manager**:** Garabed Simitian

Drivetrain Team
Team Lead: Ashley Bermudez
Alejandro Rubalcava
Andy Garcia
Daniel Hernandez
Isaiah Arevalo
Jacob Adison
Jason Kim
Jesus Sanchez
Olivia Cade

Chassis Team
Team Lead: Luis Diaz
Caden Pak
Christian Villalobos
Daever David
Diego Valenzuela
Elizabeth Padilla
Haik Zarikyan
Jared Carrillo
Jessica Tolentino
Jocelyn Camarena
Jose Puentes
Matthew Aralar
Nathan Gabriel
Yannis Nyemeck

Transducer Deployment Team
Team Lead: Aaron Bonilla
Brandon Canedo
Dylan Davenport
Hector Torres
Marcelino Maldonado

Systems and Controls Team
Team Lead: Ryan-Matthew Dela Rosa
Brandon Maldonado
Jiego Harel Judge
Nareg Shirajian
Ori Dabach
Suzanne Fisher
Matthew Awad
Noe Diaz

Faculty Advisor: Dr. Christoph Schaal

California State University Northridge

Autonomous Non-Destructive Testing Robot

By: Ricky Chi Yam, Garabed Simitian, Ashley Bermudez, Luis Diaz, Aaron Bonilla, Ryan Delarosa, Alejandro Rubalcava, Andy Garcia, Brandon Canedo, Brandon Maldonado, Caden Pak, Christian Villalobos, Deaver David, Daniel Hernandez, Diego Valenzuela, Dylan Davenport, Elizabeth Padilla, Haik Zarikyan, Hector Torres, Isaiah Arevalo, Jacob Adison, Jared Carrillo, Jason Kim, Jessica Tolentino, Jesus Sanchez, Jiego Judge, Jocelyn Camarena, Jose Puentes, Marcelino Maldonado, Matthew Aralar, Matthew Awad, Nareg Shirajian, Nathan Gabriel, Noe Diaz, Olivia Cade, Ori Dabach, Suzanne Fisher, Yannis Nyemeck

I have read and reviewed this paper prior to submission to NASA MINDS.

_____ _____

Faculty Advisor Dr. Christoph Schaal Date

California State University Northridge

Acknowledgements

The CSUN American Society of Mechanical Engineers club team would like to thank Shaun Ford for his mentorship and guidance throughout this past year. Shaun graduated as a Mechanical Engineering student at CSUN and has returned to major in Computer Science. He is exceptionally helpful, and we appreciate him taking the time out of his busy schedule to provide the team with his mentorship and guidance. He has provided the team with invaluable advice and helped make everything as professional as possible.

The CSUN ASME team would also like to thank Professor Gonzales, a former graduate student and current professor at CSUN, who did research on Non-Destructive testing mechanisms for his thesis. He also provided the team with invaluable advice on the custom circuitry that interacts with the transducer to perform the tests and was incredibly supportive of our project.

The CSUN ASME team would also like to thank Troy O'Neill and Max Tchen, two undergraduate students at CSUN who are currently working on their senior design project. They provided the team with plenty of great advice on professionalism and how to stay organized. They were also excellent role models to the members on the team who look up to them in their college career.

The CSUN ASME team would also like to thank Maxwell Vitebskiy, a computer science student at CSUN, for providing the team with guidance on how to use some of the coding software needed to accomplish this project. We are very appreciative of him taking the time to teach us and pass on some of his knowledge.

The CSUN ASME team would also like to thank the ASME club at CSUN for providing a majority of the funding for the project and for providing the team with all the resources they needed to make the project a reality. The club and all its members have been extremely supportive of our team. The team operates as a club inside a club, and without the support of the rest of the club, and its board members, this project would not be possible.

The CSUN American Society of Mechanical Engineers team would like to thank their faculty advisor, Dr. Christoph Schaal, without whose support this project would not have been possible. Throughout the whole year, Dr. Schaal has been extremely supportive of the team and their design efforts. He has provided amazing guidance to the team and has been very encouraging. His feedback has help us create an amazing design, much better than we would otherwise have been able to accomplish. His feedback as taught the team many invaluable lessons and helped us all become better engineers.

And lastly, the CSUN ASME team would like to thank all the students, faculty, staff, and industry professionals who attended the teams Preliminary Design Review, and Critical Design Review. Their ideas, insight, suggestions, and critiques proved unbelievably valuable to the team and we greatly appreciate all of them for taking the time to attend and help us.

Table of Contents

Abstract

Nondestructive testing (NDT) using ultrasonic transducers is a common method of inspecting materials on large assemblies to detect internal damage without having to take apart the assembly or cut into the part. This technology is becoming even more relevant as new composite materials are developed as they can experience several types of internal damage, such as delamination and disbands. As a result of the increasing need for NDT, a practical method of conducting such tests is needed. In this project, a robot that can traverse the surfaces of air and spacecraft is developed that can perform NDT. A system engineering approach is used in the design process of the robot to manage the project. Due to limited manufacturing capabilities, 3D printing technologies are heavily utilized, and its limits are explored. The project schedule and delays are discussed as well as the System Requirements Review, Preliminary Design Review, and Critical Design Reviews that were conducted. Finally, the robot is manufactured and tested.

1 Introduction

1.1 Motivation and Objectives

Over the years, composite material technology has been advancing and their use in industry has been on the rise. These composite materials offer many advantages such as having a high strength-to-weight ratio [1]. As these technologies continue to advance, composites find their way into many critical applications such as air and spacecrafts, and are increasingly found in structural components. However, composites are susceptible to internal damage that cannot be detected with visual inspection such as delamination and disbands [1]. If such internal damage is not detected, it can lead to catastrophic failure.

One method of detecting internal damage in materials is ultrasonic non-destructive testing (NDT) method. Currently, most NDT is done by a human operator, who is prone to making mistakes depending on their training [2] [3]. To make the process of conducting NDT on the surface of an aircraft or spacecraft more time efficient and reliable, it is necessary to have robots that can conduct the test. Such robots can prove to be extremely valuable to organizations that operate large aircraft or spacecraft that makes extensive use of composite materials, such as NASA. Programs such as the NASA Artemis program have made sustainability and reusability a primary goal [4] [5], and a big part of achieving this will be the safe reuse of space vehicles. Having a way to test for internal damage effectively and efficiently will be critical to achieving sustainability and reusability. In this aspect, a robot that can traverse the surface of the spacecraft and autonomously perform NDT will be extremely useful to NASA, the Artemis program, and any other program or organization that requires safe reusability and sustainability in their air and spacecrafts.

In addition to the increasing use of composite materials, one other technology area that has advanced in recent years and become more widely available and affordable is additive manufacturing, also known as 3D printing. This new technology allows for rapid prototyping, development, and cost-effective manufacturing of parts that would normally not be possible with conventional manufacturing techniques. This new technology can help develop new light weight robots with unique design characteristics much faster and allow new robotic technologies to be developed.

The focus of this project is towards developing a robot that can perform NDT on spacecraft surfaces. The robot is intended to be operated before launch to ensure that spacecraft is safe to operate, or after a return to Earth to ensure it is safe to reuse. Due to the limited manufacturing capabilities of the team, 3D printing is utilized in the design and development of the robot. The limits of 3D printing are including the complexity and types of the parts that can be printed, and the challenges of using it. Throughout the design process, a System Engineering (SE) approach will be utilized to make the design process as smooth as possible and create the most effective solution.

2 Project Management

2.1 System Engineering

Developing an NDT robot that can traverse all surfaces on a spacecraft and have limited autonomous capabilities is a complicated design challenge. To help meet these challenges and make the design process more efficient, a system engineering approach was utilized. Firstly, after the system requirements review (SRR), described in detail in Section 2.2, the team broke down the full robot system into several system hierarchy levels and subsystems. This made the design process much more efficient since each subsystem would handle a specific set of requirements for the robot and a dedicated sub-team of engineers would work on designing that subsystem. Figure 1 shows the subsystems and system hierarchy levels of the robot.

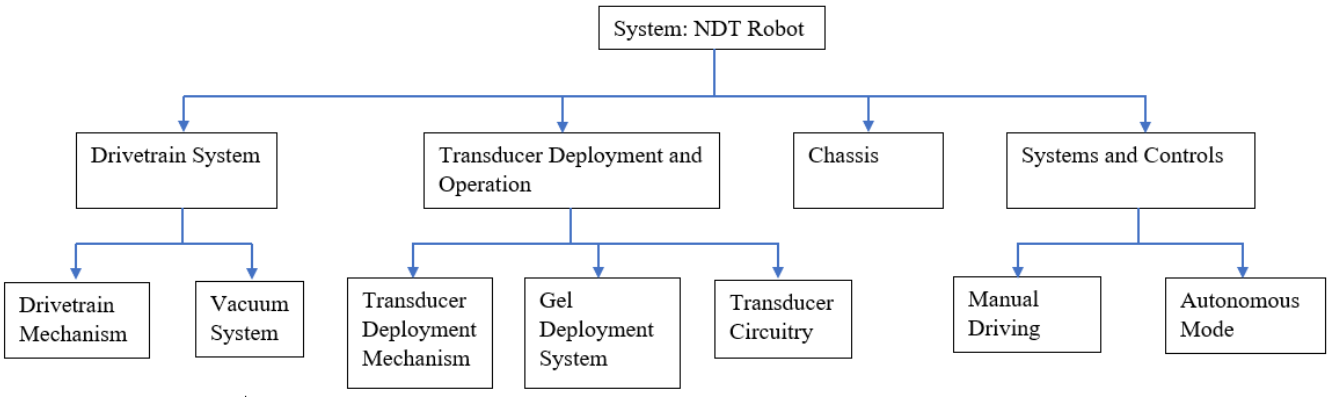

Figure 1: System hierarchy levels and subsystem breakdown of the robot.

Throughout the design process, several design reviews were conducted, including a Preliminary Design Review (PDR) and Critical Design Review (CDR). For these design reviews, the team presented the most recent progress to our faculty advisor and an audience that included students, faculty, staff, and professors from CSUN and industry professionals. Trade studies conducted using design matrices were presented during PDR and the final design was presented during the CDR. The external reviewers present at these presentations provided a new perspective to the design and provided valuable criticism and feedback that helped improve the robot. After each design review, the team made improvements and adjustments based on the advice and feedback received. Some of the changes made due to these design reviews is discussed in detail in Section 4, Robot Design.

2.2 System Requirements Review

During the SRR, the requirements for the robot were finalized and the full scope of the project was determined. In accordance with the SE principles, the requirements were set to be specific, meaningful, and measurable.

It was determined that the robot should be small and lightweight so that multiple robots can operate on the surface of the spacecraft simultaneously without damaging the structure due to the weight of the robots. It was determined that the size of the robot shall be 20 cm x 20 cm x 15 cm (L x W x H) and the robot shall weigh 2 kg (19.6 N) or less. To avoid damaging the spacecraft surface, only soft contact with the surface shall be allowed, meaning things such as metal wheals cannot be used. To be able to perform measurements on most spacecraft surfaces, the robot shall be capable of driving across most surfaces of a spacecraft, including up to a 90° slope. The robot must not use any external power supplies or be connected to external devices such as external vacuum pumps or air tanks. The robot shall be capable of operating for a minimum of 60 minutes.

The ultrasonic transducer that will be used is the B-454, which will be lent to the team by our faculty advisor. The use of this transducer adds some additional requirements for how the sensor will be deployed, and how signals will be sent to and received from the transducer. When deploying the transducer, the force on the transducer shall not exceed 2.5 N +/- 0.3 N. A custom circuit that shall convert PWM signals to a Hann Windowed sinusoidal wave will be needed to send signals to the transducer. A custom circuit that shall receive signals from the transducer and amplify it will also be needed. Lastly, because the B-454 transducer is a contact transducer, an ultrasonic gel must be deployed in the location where the transducer will touch the test surface.

The robot shall have two operating modes. There shall be a manual mode for use in all situations. In this mode, the robot shall be controlled via a remote control. The robot will also have a limited autonomous mode that can function on relatively flat surfaces with well-defined edges. In autonomous mode, the robot shall localize on the spacecraft surface and autonomously find the test locations using coordinates sent to it by either an external algorithm (not developed by our team) or sent by a human operator. Once at the test location, the robot will autonomously conduct the test.

Several assumptions about the operating conditions of the robot will be assumed in development. Firstly, the robot will be operating on a clean surface (one that has been cleaned for inspection). Secondly, it will be operating on a stationary spacecraft that is either about to be launched into space or has just returned and is being inspected for reuse. The robot is not intended to be used in space. Finally, the environment the robot will be operating in will be an indoor hanger, or similar environment.

2.3 Project Schedule Overview

The project has several major deadlines that must be met. The deadline for delivering the robot is April 30 0f 2021 when the final demonstration of the robot and its capabilities are set. The project lifecycle will extend until mid-May to give the team time to close out the project after the final demonstration. A preliminary design review paper was due on December 14, 2020 and a system engineering paper documenting the design of the robot is due on March 26, 2021. These deadlines are imposed on the team by NASA MINDS and must be met for a successful project completion.

In addition to the external deadlines, several internal deadlines for important milestones were set by the team. The PDR presentation to the faculty advisor and other guests was held on December 4 and the CDR presentation was held on February 15. An Operational Readiness Review (ORR) is scheduled for April 16. Manufacturing was planned to begin in mid-February. The full Gantt chart can be seen in Figure A.1 in the Appendix. Items in green represent planned schedule tasks that were completed on time and light tan color represents the planed completion date for tasks that were not completed on time.

Throughout the project, weakly meetings for the whole team were held to discuss the design of the robot and for all sub-teams to provide updates on their progress. These meeting also allowed all sub-teams to communicate on the interfaces between subsystems. The project manager and team-leads also conducted a weekly meeting to ensure that everyone is meeting deadlines and evaluate changes to the schedule that needed to be made due to delays and setbacks. Finally, each sub-team held biweekly sub-team meetings to design the individual subsystems each team was responsible for.

Due to several delays and setbacks in the design process, the planned timeline for manufacturing got shifted from mid-February after the CDR to the start of March. The delay was caused by several modifications to the design that needed to be made after CDR, and the manufacturing process taking longer than scheduled due to manufacturing and 3D printing difficulties, discussed in Section 4. The current schedule is now such that one prototype will be completed by the end of March, with the second prototype being completed by April 16, 2021. Several critical systems will be tested before March, but much of the system verification needed to be pushed back to the start of April. These delays are reflected in the Gantt chart and are indicated with the dark tan colors. Expected delays in the future are indicated with the blue color.

2.4 Budget and Cost of Project

The total budget available for the project is $5,000.00. $3,500.00 is provided by the American Society of Mechanical Engineers CSUN chapter, and the remaining $1,500.00 is provided by NASA MINDS after approving the team's PDR paper. Two robots will be manufactured as prototypes. It was determined that the cost of a single robot should be $2,000 with $500 set aside for unexpected expenditures. The total projected cost for 1 robot is $1,670, an increase from the $1,300 projection from PDR. Table A.1 in the Appendix shows the items needed and the cost for one robot and Table A.2 in the Appendix shows the total expected spending for the project. The increase in cost of the robot is due to several upgrades made to purchased components. As of this writing, one of the two prototypes of the robot have been manufactured, and the total amount spent by the team is $2,450.08. This includes cost of materials purchased for research and testing, materials for the first robot, and shipping and taxes. This larger than predicted amount is due to delays that resulted in a need to pay extra for fast shipping. However, based on the amount spent so far, the team is set to complete the project within the allocated budget.

3 Nondestructive Testing

3.1 Ultrasonic Testing Methodology

The NDT will be performed by the B-454 contact transducer. The transducer is a piezoelectric device that takes voltage input and converts the voltage signal into a mechanical wave. It can also take a mechanical wave and convert it into a corresponding electrical signal. However, the B-454 can only either transmit mechanical waves or receive mechanical waves. To perform testing, it is necessary to have a minimum of two contact transducers, one transmitting waves, and one receiving waves, to gather data. Furthermore, each transducer needs its own circuitry to operate, a transmitting circuit and receiving circuit. Using one transducer and a switching circuit, such as the one in [6] was also considered, but this was deemed too impractical due to the complexity of the circuit.

Due to the need for two transducers to conduct the test, it was decided that two robots would work in tandem to conduct the test. One robot would carry a transducer combined with the appropriate circuitry to send signals, while the other robot would carry a transducer combined with the appropriate circuitry to read measured signals from the transducer. This multi robot approach would also lend itself to expandability of the system, where multiple robots can be carrying the equipment for reading signals and a swarm of robots can be used to test an entire surface more efficiently.

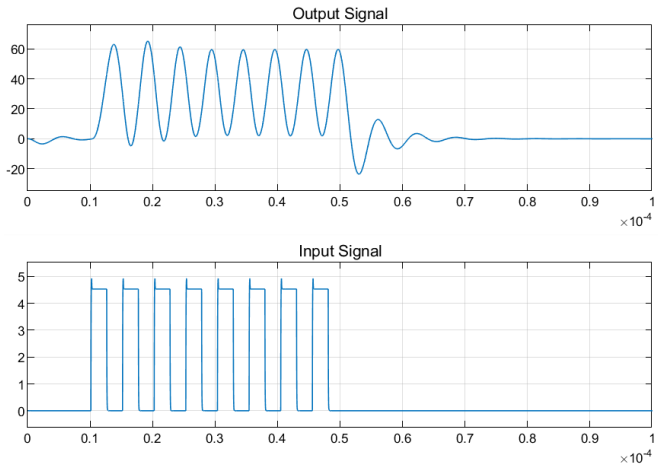

Figure 2: Input PWM signal after the AND gate (bottom) and output sine wave (top) for the signal amplification circuit.

3.2 Custom Transducer Circuitry

The Signal Amplification Circuit will take a 3.3 V to 5 V PWM signal at 197.5 kHz with a 50% duty cycle generated by a microcontroller, and convert it to a 50 V to 100 V peak-to-peak voltage Hann Windowed sine wave to supply to the transducer. Figure 3 shows the Signal Amplification circuit model in Simscape. The first section of the circuit contains an AND gate that takes the PWM signal and ANDs it with a second PWM frequency at 10 kHz with a 40% duty cycle to accurately control when the signal is turned on and off. The final input signal after the AND gate is shown in the bottom graph in Figure 2. The signal is on for approximately 40 µs. The second stage of the circuit takes the PWM input

and amplifies it to an 18 V square wave. This is accomplished with an 18 V DC source and a combination of transistors and MOSFETs. This section of the circuit is based on the amplification circuit presented in [3]. The last section of the circuit uses a third order low-pass filter with a cutoff frequency of 200 kHz to convert the 18 V square wave into a sine wave. Lastly, a transformer boosts the voltage to the final desired voltage of over 60 V peak-to-peak. The final output is shown in the top graph in Figure 2.

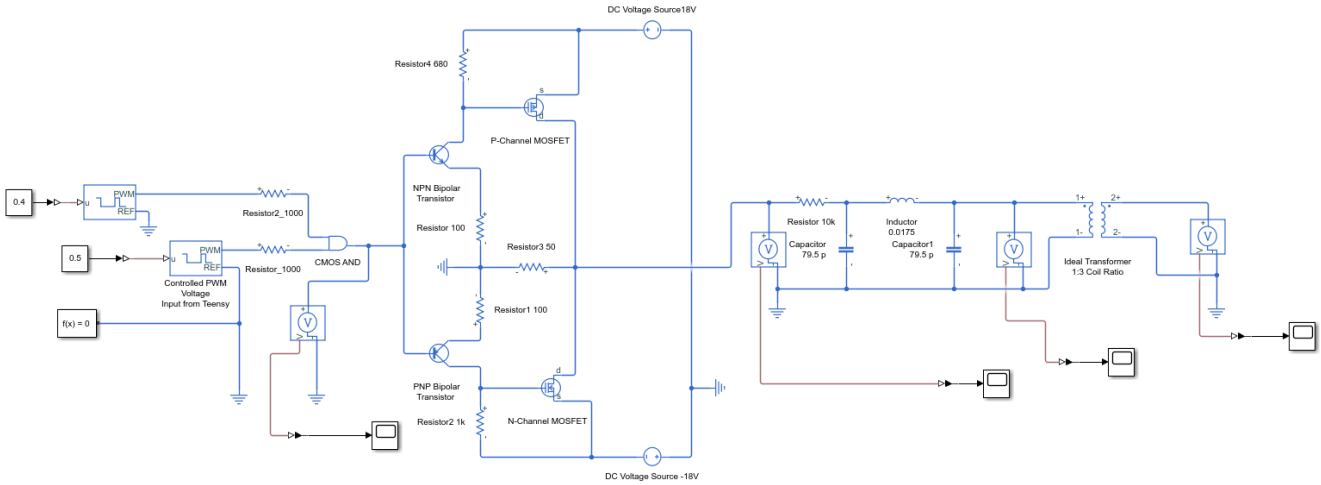

Figure 3: Simscape model of the signal amplification circuit.

From Figure 2, we can see that the output signal generated by this circuit is not the Hann Windowed sine wave the team would have liked to achieve. Within the time constraints of the project, we were unable to generate the desired wave. Several circuit designs were attempted to apply a Hann Window to this sine wave, however, the best signal we were capable of achieving is shown in Figure A.2 in the Appendix, and the corresponding circuit is shown in Figure A.3 in the Appendix. Although this signal looks promising, due to our lack of understanding on what the signal is, we decided not to use it. However, although the team was not able to generate the Hann Windowed sine wave, the regular sine wave is still an acceptable signal for the transducer, although not the ideal signal we would like to have transmitted and can still be used in the final product to conduct the NDT and gather valid data.

The second circuit is the Signal Conditioning Circuit. It will take up to a 0.3 V peak to peak voltage signal generated by the transducer and amplify and condition the signal to be read by the microcontrollers on the robots. The circuit is based on the signal conditioning circuit presented in [7] and [3]. The circuit consists of 4 stages. The first stage has 2 diodes that clip the voltage in situations where there is a voltage surge, such as when the transducer is bumped, to protect the rest of the circuit [7]. The second stage of the circuit is a high pass filter with a cutoff frequency of 994.72 Hz. This will filter out low frequency noise due to temperature drifts and power supply oscillations. The third section of the circuit is a noninverting amplifier with a gain of 11. This consists of an operational amplifier and a 100 kΩ and 10 kΩ resistor. The last stage of the circuit is a third order active Butterworth filter with a cutoff frequency of 1.25 kHz. An analog to digital converter with a sampling rate of 5

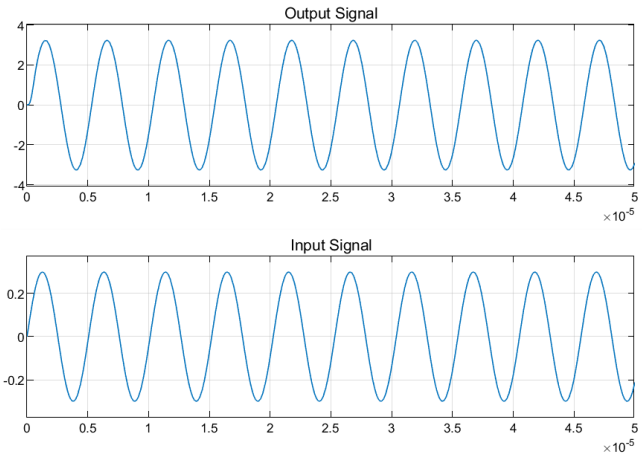

Figure 4: Input signal (bottom) and output signal (top) for the signal conditioning circuit.

M-samples / s is used to read the data from the circuit. This gives a Nyquist frequency of 2.5 kHz. The cutoff frequency for the filter was chosen to be below this number, but above 1 MHz, which is the upper frequency range of the transducer according to its datasheet, shown in Figure A.5 in the Appendix. The operational amplifiers used in this circuit should have a slew rate of at least 500 V/μs and a bandwidth frequency of at least 5 MHz. The operational amplifier used in the simulation model in Simscape is the LM7372. The Simscape model used to test this circuit, along with the input and output is shown in Figures 7, 8, and 9, respectively.

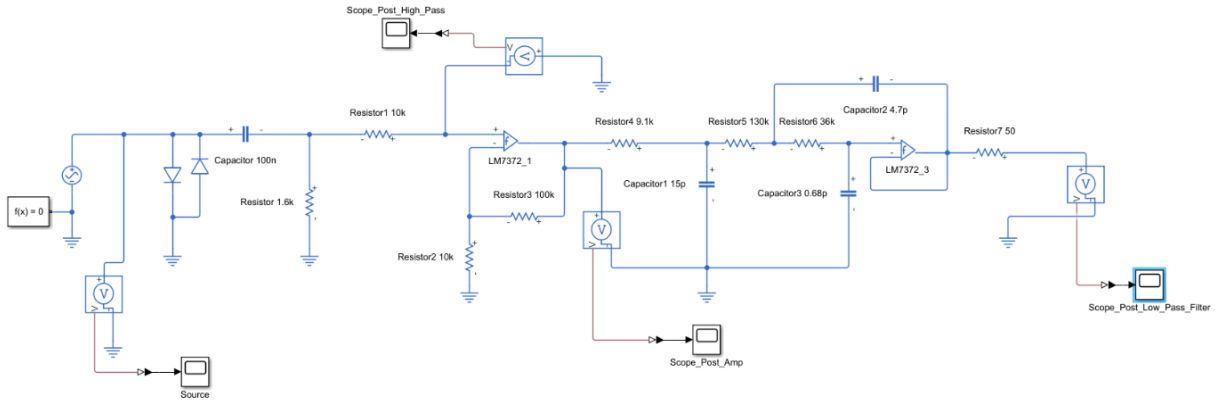

Figure 5: Simscape model for the signal conditioning circuit.

4 Robot Design

4.1 Transducer Deployment System

The goal of the transducer deployment system is to deploy the B454 Broadband Acoustic Emission Sensor effectively and safely based on the system requirements defined in Section 2.2. To accomplish these requirements, a transducer deployment mechanism and gel deployment system are needed.

4.1.1 Transducer Deployment Mechanism

The goal was to design a deployment mechanism to lower the transducer to the surface of the spacecraft. As the transducer moves down, it is required to apply a force of 2.5 +/- 0.3 N on the surface of the craft. Several design ideas were explored, shown in Figure 6. The first one was the slider crank mechanism which included a servo motor, two custom binary linkages, slider racks, screws, and a transducer holder which holds the transducer in place. The rotational motion is converted to linear motion along the z-axis. The servo was initially placed at 90 degrees while rotating 180 degrees in the clockwise direction, lowering the transducer. The second design is the dovetail slide, whose main components are a stepper motor, lead screw, a housing, and transducer sheath. This design converts rotary motion to linear motion with the help of the lead screw powered by the stepper motor. The sheath moves up or down depending on the direction that the motor is spinning. This design uses a custom lead screw that will be 3D printed rather than bough to save weight. The last design is the mini-linear actuator. In this design, the linear actuator will be oriented downward to deploy the transducer. This design includes a custom ternary linkage, two custom binary linkages with a slot, a mass weight, and a support plate. The slots on the binary linkages are designed to allow for a unilateral applied force on the transducer and wing surface. Within each design, with exceptions to the transducer, stepper motor and the linear actuator, would be 3D printed. After PDR, the plan was to use ABS as the printing material, but for reasons discussed in Section 4.4.2, the material was switched to Pro PETG.

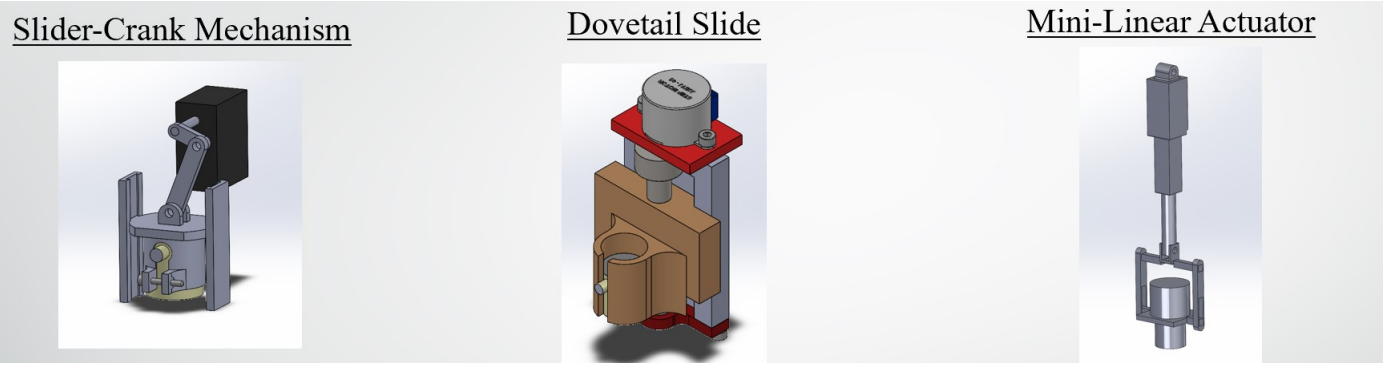

Figure 6: The 3 design options considered for the transducer deployment mechanism.

To determine an appropriate design, a design matrix was created with criteria including weight, precision, complexity, cost, size, and manufacturability. The weight was scored based on what system was the lightest since the overall goal was to keep the robot under 2-kg. The design matrix along with the results are shown in Table 1. The design which scored the highest points for transducer deployment was the dovetail slide due to its performance in cost, precision, and weight. During the time after CDR, every component of the dovetail slide design was modeled and analyzed. Motion studies performed in SOLIDWORKS showed that the leadscrew design and custom threads work in simulation. The final design is shown in Figure 7.

TABLE 1: Design matrix for transducer deployment mechanism. The dovetail slide was selected for final design.

Criteria	Max Possible Points	Slider-Crank	Dovetail Slide	Mini-Linear Actuator
Cost	25	20	23	15
Size	15	14	12	10
Manufacturablity	25	23	21	20
Precision	35	27	33	33
Simplicity	20	15	17	17
Weight	50	48	46	33
Total Points	170	147	152	128

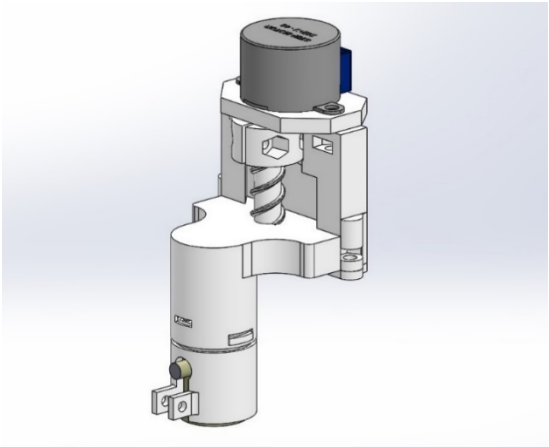

Figure 7: Finished CAD model in SOLIDWORKS of the dovetail slide design.

Manufacturing the assembly shown in Figure 7 proved to be a challenge. Printing many of the small parts proved to be difficult and several parts had to be printed several times. The lead screw and carriage proved to be challenging and required a redesign after printing revealed that the threads do not work properly. The issue was caused by the threads being too big resulting in an interference fit between the threads. After 2 redesigns, the lead screw and carriage were successfully printed and function as designed. Figure 8 shows the finished lead screw after printing.

Another factor to consider was measuring the force applied to the surface of the wing and more importantly upon the transducer. In Figure 9, the two types of force sensors that were

Figure 8: Finished 3D printed lead screw.

considered in PDR were a force sensing resistor (FSR) and load cell sensor. The FSG005WNPB Honeywell load cell contains piezo resistors that increase when the flexed under an applied force. The resistors are connected in the form of a Wheatstone bridge which behaves as a voltage divider. The load cell provides precise and reliable data that ranges from 0 to 20 N, a larger sensing range for a higher cost. The FSR sensor values are based off the proportional relationship between voltage and resistance. When unloaded (no force applied) the sensor reads 0 V and the resistance remains at the maximum value. When loaded (force is applied), the resistance decreases as voltage increases. The sensor ranges from 0.1 to 10 N and can operate within the applied force tolerance requirement of +/-0.3 N. The Interlink model 400 force sensor was selected due to low cost, great precision, and size advantages.

After the CDR, most of the parts had been purchased or entered the manufacturing phase. Testing the FSR sensor was crucial to meeting the applied force parameter. The calibration for the FSR sensor was done with the use of a gram scale and U.S quarters. Using Newton's Second Law we calculated the mass (number of quarters). The force and gravitational acceleration are known values, therefore the minimum and maximum mass required is 228 g and 280 g. LabView was selected as the calibration software and the FSR was connected to the Arduino Uno used for data acquisition. Figure A.4 in the Appendix shows the calibration curve represented by 10 data points in increments of 5 quarters each. Upon completion of the 3D fabricated models, the FSR readings are tested against varying stepper motor acceleration values. Based on these readings the acceleration can be adjusted to operate within the applied force restriction between 2.2 and 2.8 N.

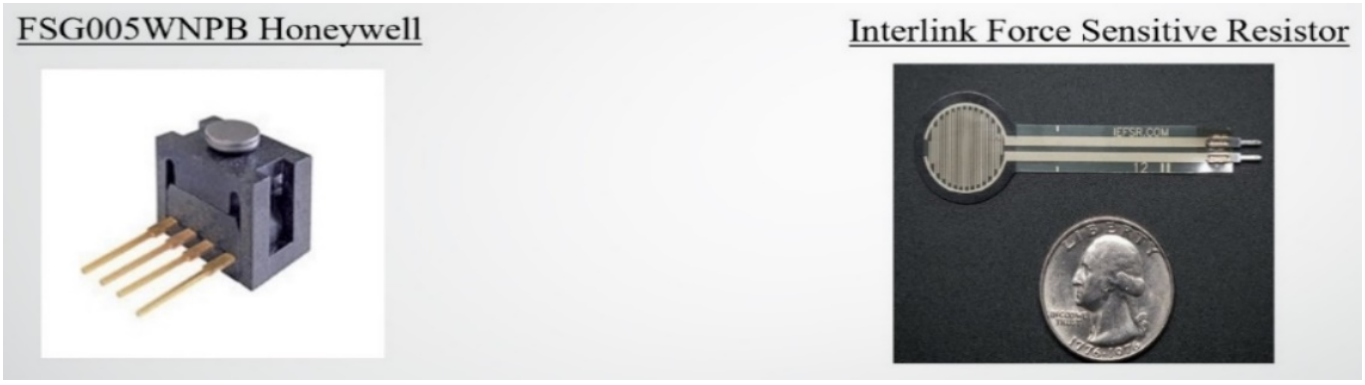

Figure 9: Possible force sensors considered for use in the sensor deployment mechanism.

4.1.2 Gel Deployment System

The gel deployment system was optimized to maximize measurement capacity while maintaining a lightweight yet versatile configuration. During the SRR it was determined that the system needed to apply 0.1 mL of ultrasonic gel to the surface, quintessential for data acquisition. Preliminary designs were based off the concepts surrounding automatic hand sanitizer devices, medical syringes, and honey pumps. Once concept sketches were developed into CAD models, the team created a design matrix to evaluate the designs. The design matrix is displayed in Table 2.

TABLE 2: Gel Deployment system design matrix. The gel syringe design was selected for final design.

Criteria	Max Possible Points	Gear Pump	Chamber	Gel Syringe
Cost	25	12	18	19
Size	15	13	8	14
Manufacturablity	25	10	23	23
Precision	35	34	30	30
Simplicity	20	12	17	18
Weight	50	42	38	41
Total Points	170	123	134	145

Due to the high viscosity of the gel and manufacturability required the gear pump was less than ideal. In addition to precision the system would need to operate 90˚ shifted from its normal orientation. An accessible storage tank paired with a positive-displacement pump would allow for multiple measurements and precise application. With its simple yet functional design the syringe-based model was selected as the final gel deployment design. A preliminary model is represented by Figure 10.

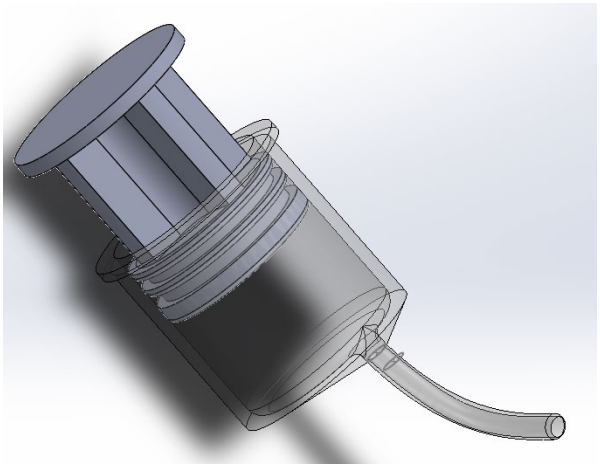

Figure 10: Pre PDR model of the Gel Syringe design in SOLIDWORKS.

After completing the PDR presentation and report, the team began refinement of the models. Refinement consisted of modeling a driving mechanism for the plunger, assigning dimensions in collaboration with the Chassis team to determine final positioning and fabricating prototypes. Initially a linear actuator was suggested as the driving mechanism, but it occupied significant volume and lacked precision. The stepper motor, like the one used in the transducer deployment mechanism, served as more compact driving mechanism instead. To counter potential leaking, which could damage electrical components, the team decided to add commercial gasket rings near the base of the plunger. Due to the plunger's limited range of motion the additional rings would ensure reliability and consistency across each measurement. In the case of electrical failure, the rings would prevent air from entering the body. This also serves to mitigate gel loss out the nozzle until the failure can be resolved.

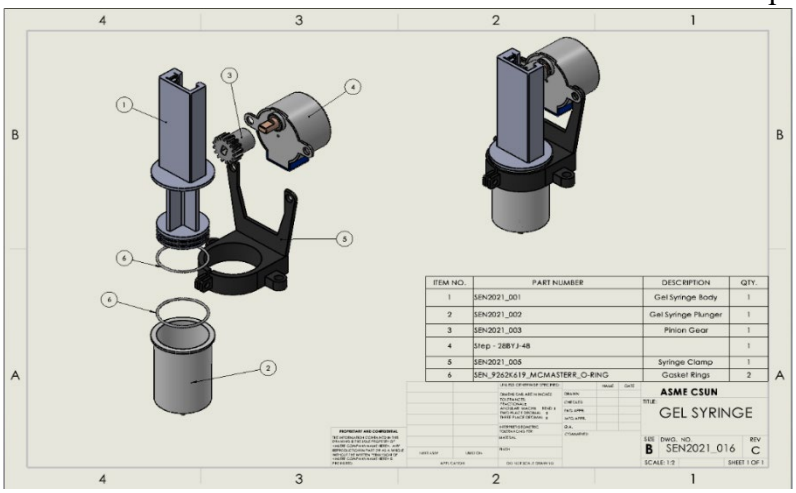

Figure 11: Final assembly drawing of the Gel Syringe Design.

The final design, shown in Figure 11, is a positive displacement pump where the gel syringe body (2) will act as a reservoir for the total amount of ultrasonic gel needed. The compact and inexpensive stepper motor (4) shall serve as the driving mechanism of this system. Utilizing a rack and pinion system, the commercially available pinion gear (3) interacts with the fabricated gel syringe

plunger (1) to control movement of the plunger. The fabricated syringe clamp (5) ensures ideal rack engagement between the pinion gear and plunger. As the plunger actuates downward, the gel is displaced out of the nozzle located at the bottom of the body. The commercial gasket rings (6) prevent leakage of gel and pressure during operation, highly desirable when the transitioning to a vertical orientation. This final model was presented during CDR.

4.2 Drivetrain System

The Drivetrain system that was developed for the robot consists of two main subsystems: the drive mechanism and the vacuum system. The requirements to meet are to have a minimum speed of 0.2 m/s, traverse up to a 90° surface, have the ability to pivot about a point, and have a precision of movement of +/- 1 mm.

4.2.1 Drive Mechanism

The drive mechanism is in control of maneuvering the robot backwards, forward and pivot on its center point. It must achieve a precision movement of 1 mm while being able to reach a speed of 0.2 m/s. Initially the team had come up with three different designs: 4 motors or 2 motors with 4 wheels, and a continuous track, the 4 motor was able to provide the highest amount of torque using 4 servo motors to drive the wheels. However, it weighed a lot, at 408 g without the motors. It also had the highest power draw taking away from the power usage requiring a larger battery adding to the total weight of the robot. The next option was using 2 motors, which provided the lightest design, however; it would fail to pivot at its center point. Lastly, the continuous track uses only 2 motors and provide the most of traction with the largest contact surface. A design matrix, shown in Table 3, was created to evaluate each design, and presented at the teams PDR. Based on the results of this study, the continuous track design was chosen.

TABLE 3 Design matrix for the drive mechanism for the robot.

Criteria	Max Possible Points	Continuous Track	4 Motor with wheals	2 Motor with wheals
Weight	50	30	10	40
Precision	35	20	25	5
Simplicity	20	10	15	10
Cost	25	15	10	20
Size	15	8	8	12
Torque Required	30	20	30	10
Total	200	103	98	97

The continuous track is a pulley driven assembly with a timing belt that gives the robot a tank like maneuverability where it can pivot in the center, allowing for accurate movements. The timing belt was made of a neoprene material, whose coefficient of friction is equal to 0.4. This gives enough friction for the mechanism to grab onto a vertical surface. The outer diameter of the pulley is 42 mm, which gives enough ground clearance for the suction cups to meet the ground while allowing it space to compress on itself. To assembly and attach the track system to the chassis a series of 3D printed parts and metal square shafts where used. Figure 12 shows the full CAD model in SOLIDWORKS.

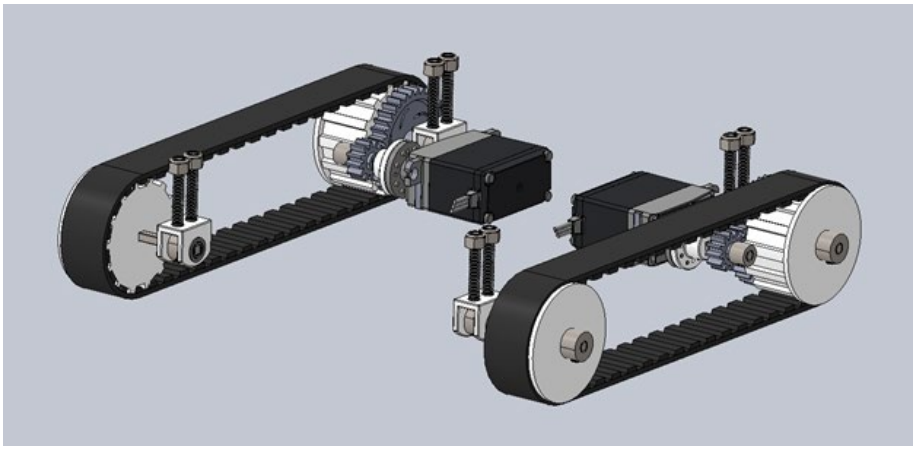

Figure 12: Drivetrain continous track CAD model in SOLIDWORKS.

To drive the pulleys, a pair of Parallax-900 continuous rotation servo motors where used. This motor was chosen due to it being low weight and containing an encoder which provides PWM feedback signal to allow for precision control, meeting the precision requirements. Testing with the motor shows that it can be accurately controlled with an accuracy of +/- 0.5° at a 95% confidence interval which translates to a movement accuracy of +/- 0.05 mm. It can produce a maximum torque of 0.537 Nm at 6.3 V, to maximize this a 3 to 1 gear ratio is attached to achieve a maximum torque of 1.611 Nm. Combining the two combination, it can provide 3.2238 Nm all at 6.3V and this can then be doubled by raising the voltage to 12V. The two motors can create a torque of 6.4476 Nm which is enough to move the entire assembled robot at a moderate speed, requiring about 6N.

The material selected for printing the parts was PETG. The reasoning for this is explained in Section 4.4.2. The settings used to print the pulley and ball bearing holders are 0.15mm layer height, 15% infill, grid infill pattern, and 0.7 mm wall thickness. These settings where selected so that the print times would be small and ensures that the small parts were strong. The ball bearing holders required sanding so that the ball bearings would have a smooth surface area to be press fit into. The metal shafts also required some grinding so that it fit into the ball bearings, both the top and bottom where grinded out by a few millimeters. Choosing not to grind on all four sides was to ensure that at least two sides of the shaft maintain its structural integrity allowing it to touch the bearing with the four conners. Since a square shaft is going into a circular bearing grinding just the top and bottom ensured the greatest contact surface for the parts.

4.2.2 Vacuum System

The vacuum subsystem has the function of allowing travel on any surface, including climbing up to a 90-degree angle. It consists of four suction cups, tubing, connectors, and a vacuum pump. The design is based off a wall driving platform described in [8]. The Thomas 1410-0103 was chosen as the on-board vacuum pump due to its small size and power. The pump specifications can be found on Table A.4 in the appendix. Initially, an inexpensive vacuum pump with similar specifications was used for testing to ensure the design concept was possible. Compared with the test pump, the Thomas pump was more expensive, but is of better quality and more powerful. The use of the inexpensive pump allowed the team to test without the worry of possibly damaging an expensive pump.

The suction cups chosen are single bellow cups made of polyurethane. They were chosen because testing revealed they performed better than the flat suction cups design. The single bellow cups proved to have better mobility when a moving force was applied while connected to a vacuum. The single bellow design allows for suction cups to perform better on uneven surfaces and can compensate for small height differences that the robot may encounter. The dimensions of the suction cups are 42 mm in diameter, 22.4 mm in height, and a collapsed height of 12.5 mm. The diameter of the suction cups was determined by considering the amount of space at the bottom of the chassis and the weight they could hold on a vertical surface. To decrease friction and allow movement while the vacuum system is turned on, low friction Teflon tape was applied to the bottom of the suction cups. Through testing, the friction coefficient of the Teflon was determined to be

0.416. Figure 13 shows the vacuum system assembly in SOLIDWORKS. The full assembly shows the design in a two-by-two formation connected by hard tubing, couplings, and cushion washers.

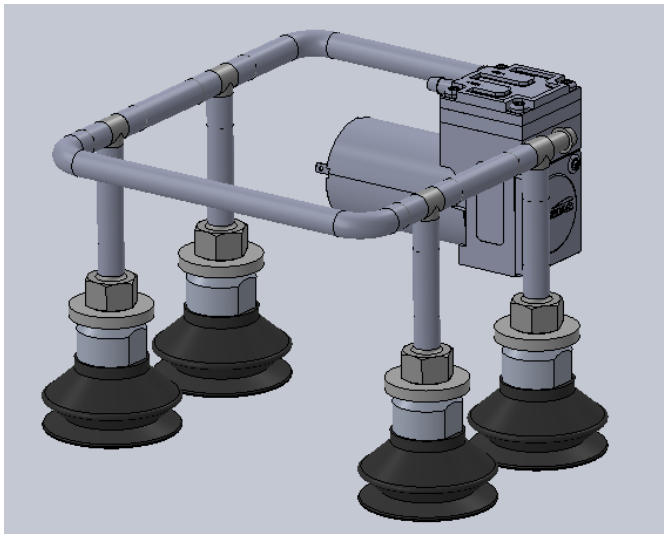

Figure 13: Drivetrain vacuum system CAD design in SOLIDWORKS.

During initial testing, the vacuum system was assembled using Tygon Thermoplastic Tubing. This soft tubing was used initially because of its flexibility. However, once the vacuum was turned on, the tubing was too soft and collapsed in on itself, making the tubing ineffective. Instead, the soft tubing was replaced with hard tubing. The testing showed that the flexible tubing is not needed and a stiffer material could be used that was stiffer, yet workable enough to be routed and changed as needed.

Initial testing of the system with 1 suction cup and the inexpensive vacuum at 12 V revealed that while moving, an absolute pressure of 604 +/- 10 hPa at a 95% confidence level is maintained in the vacuum system. Based on this, and the area of the suction cups, an average lifting force of 15.7 N is obtained. With 4 suction cups, it is expected that our lifting force will be 62.8 N, well above the minimum of 20 N of force needed to hold up the weight of the robot. Further validation of the system is discussed in section 4.7.

4.3 Systems and Controls

The systems and controls sub-team is responsible for the controls of the robot, the wiring, and the limited autonomous capabilities. This includes the manual driving and autonomous operation subsystems shown in Figure 1.

4.3.1 Overall Systems and Controls Architecture

The main control board for the robot is the Raspberry Pi 4 with 8 GB of RAM. This will serve as the main brain of the robot. Connected to the Raspberry Pi will be 2 Arduino Nano Every boards using serial communication that take commands from the Raspberry Pi and execute them. The use of the 2 Arduino boards allows the addition of analog ports and increases the number of pins available for connecting sensors to the robot. In terms of sensors, the robot will contain voltage sensors, pressure sensors, edge detection sensors, and proximity sensors.

Edge detection sensors will be necessary to prevent the robot from falling off surface and for the edge detection and coordinate system creation described in Section 4.3.2. Several potential sensor choices were considered for detecting the edges of the surface the robot is operating on and are summarized in the design matrix, shown in Table 4. Based on this design matrix, the VL6180X ToF sensor was chosen. In conjunction with the ToF sensors, the Intel RealSense T265 camera was included due to its internal measurement unit (IMU) and position tracking capabilities that will be useful for creating an internal map of the surface.

TABLE 4: Design matrix for picking the edge detection sensors.

Criteria	Max Possible Points	Ultrasonic Sensors	IR Sensors	ToF Sensors
Weight	50	45	30	40
Precision/Accuracy	35	30	25	35
Simplicity	20	20	20	20
Cost	25	20	25	15
Range	25	25	25	20
Size	15	5	10	15
Power Consumption	30	25	20	30
Total	200	170	145	175

Several potential sensors were also considered for the proximity detection sensors. The proximity detection sensors are necessary to prevent collisions with other NDT robots that may also be operating simultaneously on the spacecraft surface and prevent collisions with structures on the spacecraft. The design matrix for the proximity sensors is shown in Table 5. Based on the results of this design matrix, the ultrasonic sensor was chosen.

TABLE 5: Design matrix for proximity detection sensors.

Criteria	Max Possible Points	LIDAR	Ultrasonic Sensors	Camera
Weight	50	15	45	45
Precision/Accuracy	35	30	25	35
Simplicity	20	15	20	10
Cost	25	5	25	20
Range	25	25	15	20
Size	15	5	15	10
Power Consumption	30	20	30	10
Total Points	200	115	175	130

To power up the robot, there will be three different internal power sources. To power up the Raspberry Pi, the robot will use a MakerHawk power management board with the use of two 18650 batteries. The Raspberry Pi will power the Arduino Nanos and the sensors connected to the Arduinos. Lastly for the pump and motors, a mixture of Li-On batteries in parallel and series will be used. Table A.3 in the Appendix shows the max current drawn by each component being powered by a power supply. Based on this data, calculations indicate that the MakerHawk battery supply will have an operating of 2 hours. The batteries powering the Parallax Servo motors for the drivetrain mechanism will supply 7.4 V and has a predicted operating time of one hour. Lastly, the battery pack for the vacuum will be supplying 11.1 V and will last for approximately 6.6 hours. Based on these calculations, the robot operating time will be a maximum of 1 hour, as the system requirements dictate.

4.3.2 Autonomous Edge Detection and Coordinate System Creation

The autonomous edge detection and edge following process requires a specific hardware configuration of the VL6180X ToF sensors. In Figure 14, the configuration of the sensors is shown. The sensors will be placed vertically facing the surface that the robot will be operating on, this way the sensors will be able to detect the edge of the surface without the robot reaching a critical point and potentially causing a tip over.

The two main algorithms that will be operating this robot will consist of an edge finding process and an edge following process. The edge finding algorithm will be executed prior to the edge following algorithm. In which the edge finding algorithm will require the six ToF sensors to passively scan the environment until it is triggered by an event such as a no convergence/Off surface. Since the six ToF sensors will have designated positions on the robot, the sequence at which the events will occur, combined with the IMU, can help us determine the current orientation of the robot. The algorithm will then adjust the robot in the correct orientation and will proceed to the edge following algorithm. Figure 15 is a representation of this process.

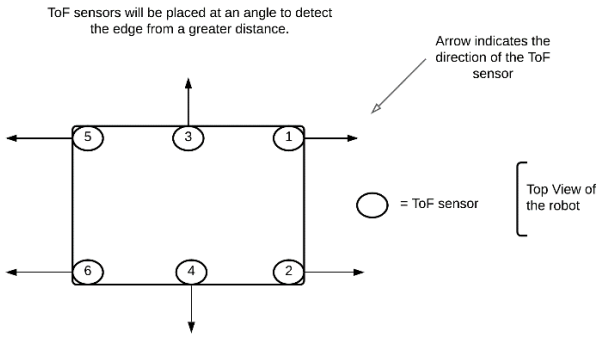

Figure 14: ToF locations on the robot and the direction they point. Sensors 1 and 2 are at the front of the robot.

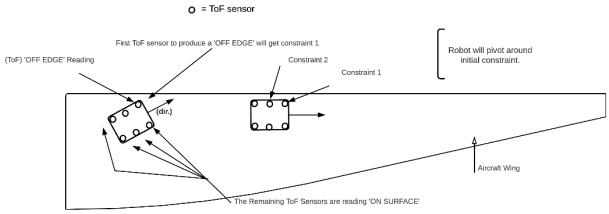

Figure 15: Diagram of ToF algorithm.

4.3.3 SLAM Algorithm

SLAM algorithms are used to determine a robot's position while simultaneously creating a map of its local environment. SLAM algorithms are implemented where traditional positioning systems such as GPS will not be able to provide sufficient data. For localization and mapping to work effectively the robots pose data must be estimated from significant landmarks, examples of these landmarks can be fixed 3D obstructions, whether it is geological landmarks or a local confined environment, such as walls or designated roads/paths. In our specific application the "significant landmark" is simply the absence of one. As it was discussed in section 4.3.1 the ToF (Time of Flight) sensors will create the boundaries of the potential test area by completing the edge following algorithm. Once the boundaries have been determined, a coordinate system will be established. A critical component of a SLAM algorithm is the ability to accurately visit/revisit a desired point in the environment it is scanning. To achieve this, once the robot has completed all the prerequisite algorithms it will reinitialize and recalibrate the tracking module to the new coordinate system. Since the robot will be

generating a digital boundary driven by a physical geometry, the robot will know to operate within the generated boundary. The rudimentary SLAM algorithm will be controlled by the Intel RealSense T265 Camera and Track Module. This module has an effective sensor suite on board that contains stereo vision cameras, six-degrees of freedom IMU, and a vision processing unit (VPU). Applying sensor fusion techniques and principles, passive, and active communication between the ToF and the tracking module will be established.

4.3.4 Manual Driving Mode

To manually operate the robot, a PS4 controller will be used. This controller will be capable of controlling all systems on the robot. Such operations are made possible by connecting the PS4 controller via Bluetooth to the Raspberry Pi. Within the Python and C++ code, the Raspberry Pi then sends data via serial communication to the Arduino when pressing buttons or using the analog sticks. The Arduino then reads the serial data sent from the Raspberry Pi and performs the designated tasks based on the inputs from the PS4 controller.

Starting with moving the robot, the left and right analog sticks of the PS4 controller will be controlling the left and right servo motors, respectively. For example, if the left and right analog sticks are held upwards, then the robot will move forward, while holding them downwards will cause them to move in reverse. Turning can be accomplished by either holding one analog stick forward and one analog stick backwards. A right turn would require the left analog stick pushed forward and the right analog stick pulled back. The opposite is true for a left turn. To control the gel and transducer deployment system, the D-pad of the PS4 controller will be used. If the D-pad is pressed downward, then the transducer will be deployed. while Up on the D-pad will retract the transducer. The gel system also utilizes the D-pad, using the Right to deploy the gel syringe, and using the Left to retract it. To control the vacuum with the relay, the O-button will be pressed to turn it on, and the X-button will be pressed to turn it off.

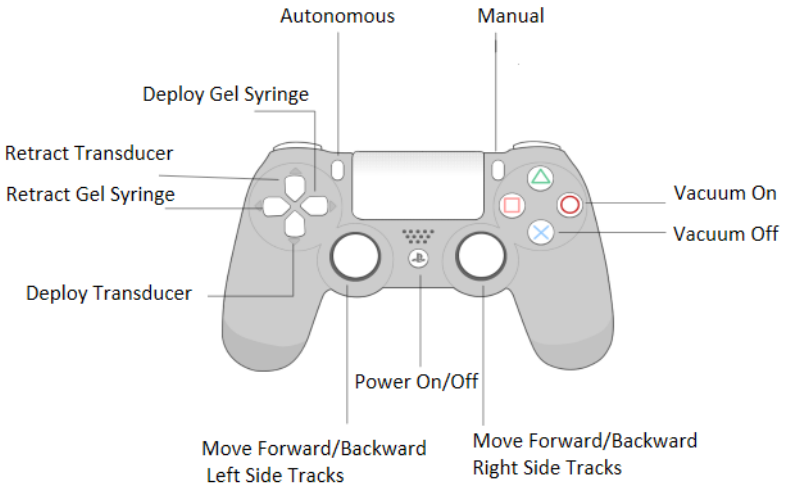

Figure 16: Remote controller button layout for the manual control system.

4.3.5 System Monitoring

To monitor and control the robot as it performs its operations, creating a Graphical User Interface, or GUI, was one method proposed to do so. As part of the design, the GUI would display parameters such as the battery life of the robot as well as display the map the Intel RealSense camera would be creating in real-time. This would also allow the user to control certain features of the robot such as turning the vacuum system on and off as well or switch between manual and autonomous mode. Ultimately, it was decided that the GUI would not be implemented for the current iteration of the robot as the systems team's focus had shifted to spending more time on programming the robot. However, developing a GUI could potentially be brought back in future models.

The command prompt from the Raspberry Pi was used throughout the programming process to give feedback and to communicate with the Arduino and the Pi. The serial monitor of the Arduino IDE was used to communicate between the Pi and Arduino. Serial communication allows for a straightforward and faster transfer of data.

4.4 Chassis

The purpose of the chassis is to contain all the components of each subteam. To do so, it must maintain its structural integrity and survive minor impacts from falls, and collisions, while remaining lightweight. The chassis sub team was also tasked with performing materials research for 3D printing for the whole robot.

4.4.1 Overall Chassis Design

The chassis team first began with 3 separate designs. They were a cubic, birdcage, and pyramid design. Each had separate focusses of balance, centre of gravity, and ability to recover, respectively. Using these sketches, the team used SOLIDWORKS to give proper dimensions in the model using the maximum of 200mm x 200mm x 150mm (L x W x H). Due to the teams limited manufacturing capabilities, the decision was made early on to 3D print the entire chassis.

To test these designs, Finite Element Analysis (FEA) using SOLIDWORKS Simulation was performed. This analysis would indicate where forces would be applied to the model and what level of extremity is applied to any given surface. The FEA results for stress and displacement will not be accurate because the model does not take into consideration the infill density and the anisotropic properties of a 3D printed part. However, these results were still acceptable as the desired information was the locations of potential failure, instead of a convergence value for stress. These results shows that it would be possible to strengthen the design either by adding supports or reshaping the model.

While performing FEA, half-sized prints were 3D printed to ensure the printers learn the limitations of the printers in use, as well as have physical models to test the physical features in the designs to see how they differ from the simulations. When printing these models, different approaches were used to see if the orientation of the print would affect the surface finish of the model in anyway, it seemingly did not. The birdcage design gave the team the most issues while printing. It could not withstand the force of pulling off the printing supports without snapping off. This testing revealed that excessively thin supports should be avoided and helped the team learn the limitations of 3D printing for structural use. Using the FEA results, the physical prints, and a few other factors the cubic design was chosen as the design to proceed with.

TABLE 6: Design matrix for the possible chassis designs.

Criteria	***Max Possible Points***	***Cubic***	***Pyramid***	***Bird Cage***
Weight	50	36	36	44
Cost	20	15	16	16
Manufacturablity	30	26	26	26
Simplicity	20	18	14	10
Size	40	36	38	32
F.O.S. of 1.2	40	34	32	18
Total Points	200	165	162	146

After PDR, the goal was to decrease the weight and begin CAD assembly with the other sub-teams. This involved making many edits to the body such as adding pillars for the TOF sensors and adding cages for the ultrasonic sensors. While making this edit, constant FEA was run to see if any changes would drastically change the integrity of the chassis. The main modification involved splitting the chassis in half horizontally. This was done to add ease in assembling the project and adding the pillars for TOF sensors blocked the original entry. This also was a helpful change when printing since having two parts means the top and bottom halves

can be oriented sideways to make the printing process easier, shorten the time and decrease the number of supports. Once the CAD was finalized, there was one final set of FEA to run which is an extreme force of 2000N to test the limits of the model. As shown in Figure 17, the majority of the force would lie towards the center of the top layer, the supports would not cave in, and the interior would not take the impact when falling and impacting the ground with this force.

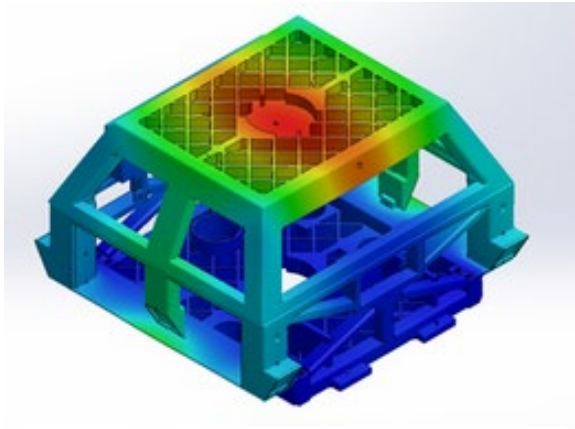

Figure 17: FEA results showing where the highest stresses are located in the chasses. Magnitude of stress values not shown.

Following the CDR, the chosen material was changed from ABS to Pro PETG due to various disparities between the materials. The main disparity being that ABS would be a potential health hazard to print on a home printer, whilst Pro PETG would not have this issue. Another final edit made was the change in material for the bolts holding the two pieces together. This was because steel would add much external weight, when there would be no need for such a strong material for something receiving minimal forces. With these additions made, the chassis was then set to begin being manufactured.

The bottom half of the chassis was printed using a 20% infill density, oriented to print from the right-hand side as the bottom to the left-hand side on top and took a total of 90 hours and 20 minutes to fully print. This print came out rather sturdy overall, with a bit of stringing on the overhangs. There was one massive stringing clot on the back of the left hand TOF sensor, luckily it did not affect the actual beam and was fixed with a bit of sanding. The overhangs were also more thing than anticipated, but still functional for its purpose. The top half was also printed using a 20% infill density, printed upside down from the placement on the assembly, and took a total of 30 hours and 26 minutes to finish being printed. This print only had some minor stringing, but no major noticeable flaws. Both chassis pieces fit together perfectly, with the holes aligning up for the bolts perfectly. The final dimensions of the printed chassis were 172mm x 193mm x 126mm (L x W x H), the length and width dimensions came out perfectly as designed, while the height shrunk to 24 mm and met the requirement of weighing less than 5-kg. Overall, the prints were a success to be used for the physical assembly, as shown in Figure 18, and the minor issues seen in the bottom half would only need minor revisions. Moving forward, the chassis team aims to reduce the weight even further by reducing the infill to 10% while hopefully maintaining the structural integrity.

Figure 18: Finished 3D print of the chassis.

.

4.4.2 Material Selection

Initial material research concluded that Acrylonitrile Butadiene Styrene (ABS) would be the best fitted material for the chassis. The main reason ABS was chosen was because it offered a high hardness value of 97 on the R Scale, a high Izod Impact Strength of 18.8 KJ/m^2, and a high tensile strength ranging from 27.6 – 55.2 MPa as opposed to other considered materials such as Polylactic acid (PLA) and Nylon. Upon further analysis, the team found that ABS is quite difficult to manufacture as it requires an extremely high printing temperature of 230 – 260 °C and needed a heated print bed of at least 100 °C. The need for such high

temperatures could potentially in turn cause warping in the material. It was discovered that ABS can emit particles when printing which could cause long term health effects, and as the team planned to manufacture at home on personal 3D printers, it was best believed not to risk the health hazard and look for a material not as hazardous.

During the Critical Design Review, the team had received recommendation of one material, Polyethylene terephthalate glycol- modified (PETG). A more concise research concluded that generally PETG is stronger than ABS in terms of tensile strength by at least 10.8 MPa, Flexural Strength by 11.4 MPa, and yield strength by 13.7 MPa. The team also found that PETG is easier to manufacture as it requires a lower printing temperature of 230-250 °C and a heated bed temperature ranging from 50 - 80 °C. This in turn means PETG has a lower printing and heat bed temperature, the material is less likely to warp. This material also has a significantly lower thermal shrinkage of 0.3-0.8% compared to ABS's 4.3%. Lastly, PETG has lower volatile organic compounds and lower particle emissions which could cause long term health effects. Based on these findings the team decided to switch materials from ABS to PETG.

When choosing a specific company to source filament from to print the chassis, the team chose the MatterHackers Pro PETG filament. The team found that MatterHackers Pro PETG filament is significantly stronger than most PETG filaments with a yield strength of 74 MPa and a density of 1.27 g/cm³ compared to other filaments such as their regular PETG with a yield strength of 49 MPa and a density of 1.23 g/cm³, or inland's PETG filament with a tensile strength of 49MPa and a density of 1.23 g/cm³. The MatterHackers Pro filament would be adding a small amount of weight to the chassis since it is 0.04 g/cm³ denser, but the tradeoff of being able to print at slightly less infill yet have a dramatic increase in strength was more than worth the slight drop-off. The cost of this material is roughly $55 for a single 1 kg spool of this material, whereas a regular PETG spool would cost anywhere between $20-25. Due to it being within the budget, the team was able to upgrade to this material for the final chassis.

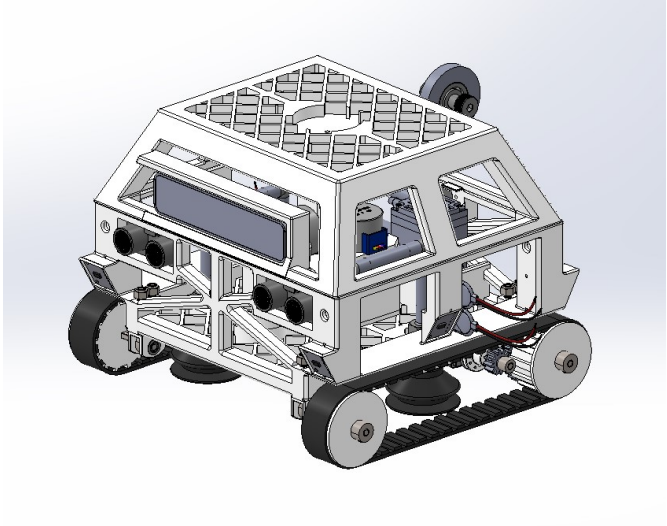

Figure 19: Full robot CAD assembly in SOLIDWORKS.

4.5 Full Robot Assembly

The full robot assembly combines all the sub-assemblies into one assembly for the entire system. When all the assemblies are combined, we can see that they interface well with each other. The full CAD model in SOLIDWORKS is shown in Figure 19.

4.6 Reliability and Safety During Operations

Several systems were put into place to monitor the performance of the robot as it is operating. Firstly, a pressure sensor will be connected to the end of the vacuum system's tubing to monitor and measure the absolute pressure in the system. This will ensure that the system remains at an appropriately low-pressure level as the robot performs its operations. If absolute pressure increases above a certain threshold, then the user will be alerted of a failure in the system via warning lights and sounds being activated. In the event that the robot was climbing up a vertical surface, it would slowly make its way down to a lower point so that the distance for a fall would be minimized if the worst were to happen, or if possible, head to a flat surface where the vacuum system will not be necessary.

To monitor the voltage supplied to the vacuum pump, a voltage sensor will be connected to the vacuum system to ensure the appropriate amount of voltage is being supplied to the system. If the voltage falls below a certain threshold, roughly found to be 5 V after performing several tests, then the vacuum system will begin

to fail, and the robot will start to lose suction. Once again, the user will be alerted by warning lights and sounds being activated. The robot would then, follow the same procedure as when pressure is lost in the system described earlier.

Between the microcontroller and the vacuum system, there will be a relay switch connected along with the voltage sensor. The relay switch will be set to the normally closed position. Given that the vacuum system and the microcontroller connected to it will have separate power supplies, if the microcontroller were to fail, the vacuum system would continue to stay on due to the closed position of the relay switch. The user would then lose the ability to turn the vacuum system on and off; however, because the vacuum system will continue to run, this will prevent the robot from falling off of the surface.

4.7 Robot Testing and Requirements Validation

Due to several setbacks and delays, discussed in Section 2.3 all systems on the robot have not be verified in testing yet. What the team has managed to do is successfully 3D print all the complex parts that needed to be printed and verified the vacuum systems and the ToF sensors. The transducer circuit designs were verified in simulation and will be validated once the PCB boards are made in April. The results of the circuit simulations were presented in Section 2.2.

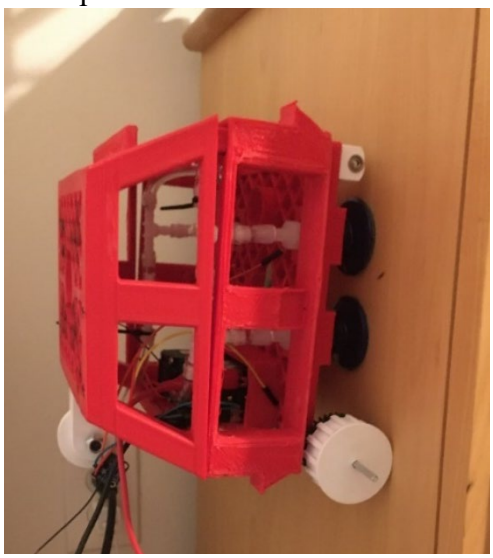

Figure 20: Robot vacuum system holding the robot up on a 90° surface.

Firstly, final testing of the vacuum system after assembly revealed that the vacuum system was indeed capable of holding up the robot weight on a vertical surface. In testing, it appeared that the optimal voltage for the vacuum was 10 V and that it could support the robot with as little as 6 V. At voltages below 6 V, the robot would remain attached to the wall, but would start to slide down. The system would not fail until the voltage dropped below 4 V. A picture of the robot during testing of the vacuum system is shown in Figure 22.

Secondly, the team has verified that the remote manual control system works. The Raspberry Pi and Arduino Nanos can receive the signals sent from the controller and perform the correct task based on the input. This was verified by setting up the circuitry and testing if the electronics performed as expected when receiving input from the controller. Due to the manufacturing delays, the system could not be testing on the full robot assembly.

Third, the team has verified that the sensors work, and the boards can read and interact with the data. The data is successfully passed between boards using serial communication. All 6 ToF sensors are reading good data and can detect edges around the robot. The team has also verified that the Intel RealSense camera performs as expected and has managed to integrate that into their system. More extensive autonomous systems have not yet been tested due to delays in manufacturing.

5 Conclusion

5.1 Current State of Project and Future Plans

As of this writing, all components of the robot have been printed and all parts have been ordered and arrived. Unfortunately, due to delays discussed earlier, the full robot assembly has only been partially assembled and only some systems have been fully tested. Going forward, the team's goals will be to finish the full assembly of the robot and test out the entire system and have a successful ORR as mentioned earlier. The team is confident that with the current state of the project, and the success it has had in validating the systems that

have been tested so far that it can successfully verify and validate the remaining requirements to be ready for the final demonstration on April 30.

5.2 Concluding Thoughts

As humanity progresses and makes progress toward Mars with the Artemis program, sustainability and reusability become ever more important goals. Creating a sustained presence on the moon and then on another planet is a difficult task that requires new technologies to be developed. Throughout this project, new technologies were explored, and many lessons were learned. Firstly, a vacuum system that can support a robot and allow it to operate on vertical surfaces where robots previously could not operate was successfully developed. Secondly, the limits of 3D printing were tested. Detailed intricate parts such as lead screws and threads were successfully printed, as well as large structural components such as the chasses. Lastly, these technologies were combined into a cohesive design to create a NDT robot that can prove extremely useful to organizations such as NASA and the Artemis program, who have made safety, reusability, and sustainability top priorities.

Bibliography

[1] A. Miranda, C. Gonzales, A. Balyan and C. Schaal, "Mobile Robotic Platform for Inspecting Aircraft Surfaces Using Lamb Waves," International Workshop on Structural Health Monitoring.

[2] C. Gonzales, "Localization and Mapping Robot using Lamb Waves for Damage and Feature Detection," California State University Northridge, Northridge CA, 2020.

[3] E. Hong, "Development of an Automated Robot for Nondestructive Testing Applications," Northridge, CA, 2018.

[4] "Forward To The Moon: NASA's Strategic Plan for Human Exploration," NASA, 2019.

[5] K. Hambleton and R. Kraft, "NASA Commits to Long-term Artemis Missions with Orion Production Contract," 23 9 2019. [Online]. Available: https://www.nasa.gov/sites/default/files/atoms/files/america_to_the_moon_2024_09-16-2019.pdf. [Accessed 12 12 2020].

[6] A. Henriquez, C. Schaal and J. Flynn, "Ultrasonic Pulser-Receiver," California State University Northridge, 2020.

[7] A. Pertsch, J.-Y. Kim and Y. Wang, "An intelligent stand-alone ultrasonic device for monitoring local structural damage: implementation and preliminary experiments," IOP Publishing, 2010.

[8] C. Venancio, E. Mar and K. Lei, "Otto - The Wall Driving Platform," California Polytechnic State University San Luis Obispo, San Luis Obispo, 2013.

Appendix

Task	10/9/2020	10/30/2020	11/6/2020	11/13/2020	11/30/2020	12/4/2020	12/14/2020	1/1/2021	1/15/2021	2/6/2021	2/15/2021	3/1/2021	3/26/2021	4/16/2021	4/30/2021
System Requierments Review															
Research Vacuum System Design															
Research Drivetrain Designs															
Research Sensor Options for Autonomous Systems															
Create Design Options for all sub teams															
30% Design Review															
Create Flow Charts for Edge Detection, AI and Localisation															
Create Design Matrix															
PDR Presentation															
Make Preliminary CAD Models															
Write PDR Paper															
Refine track system design															
Refine dovetail and gel syringe design															
Refine vacuum system design															
Lower Chassis Weight to 0.5 kg or less															
Combine sub team CADs into Full Assembly															
Test Sub-Systems and Prototypes															
CDR Presentation															
Create Libraries and algorithms in Python and C++															
Test Code and custome libraries															
Write Final Code															
Manufacture Robot															
Test Robot															
Make Poster															
Write System Engineering Paper															
Make Technical Video															
Manufacture PCB boards															
Operational Readiness Review															
Demonstrate Robot Capabilities															

Figure A.1: Gantt chart showing the planned schedule and the realized schedule for the project. Green shows tasks that were completed on time. The light Tan color represents the planned completion dates for delayed items, and the dark tan colors represent how far behind schedule. Blue represents future predicted delays.

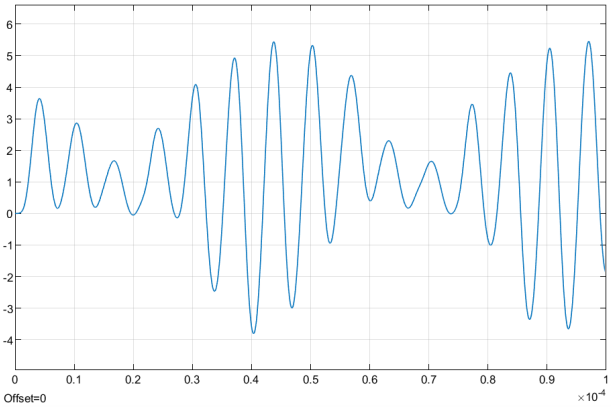

Figure A.2: This is the most promising signal the team was able to generate to replicate a Hann Windowed sine wave. It was done using an amplitude modulation circuit and a third order Butterworth filter.

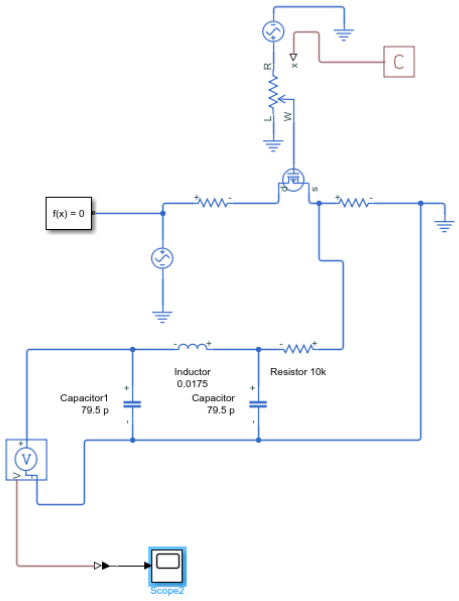

Figure A.3: The Simscape model of the circuit that was used to generate a voltage output similar to a Hann Windowed sine wave using amplitude modulation and a Butterworth low pass filter.

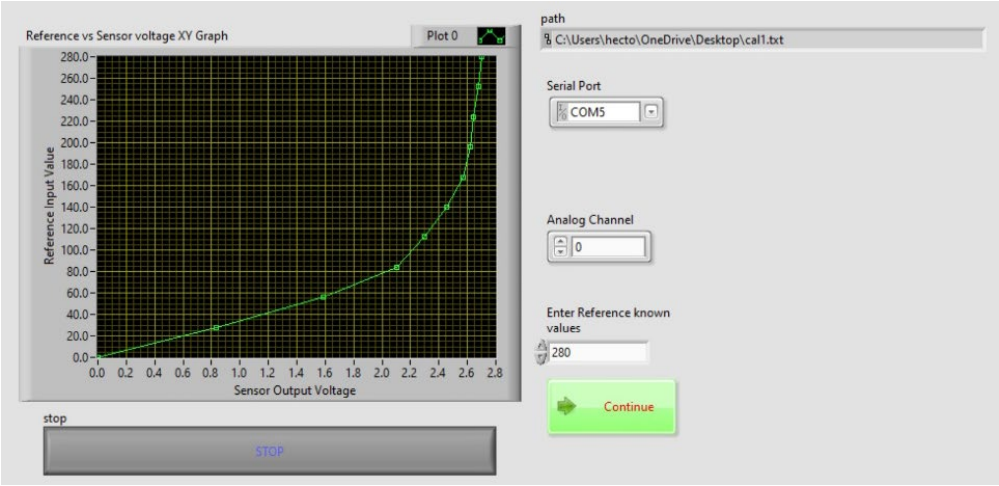

Figure A4: Calibration data results displayed in LabView.

TABLE A.1: A table of all the items needed to build one robot. The quantity for the nuts / screws / bolts was recorded as NA to avoid needing to list all the nuts, bolts, and screws bought.

Needed Items	***Quantity***	***Price per Unit***	***Total Price***
Vacuum Pumps	1	$187	$374
Tubing	1 meter	$23.49/3.05 m	$23.49
Motors	2	$30	$60
Suction cups	4	$16	$64
Suction cup connectors	4	$5.55	$22.20

Needed Items	*Quantity*	*Price per Unit*	*Total Price*
3D printing material	4 Spools	$55	$220
Raspberry Pi 4 8 GB	1	$95	$95
Arduino Nano	3	$10	$30
Time of Flight Sensors	6	$15	$90
Ultrasonic Sensors	3	$5	$15
Intel RealSense Camera	1	$200	$200
Ultrasonic Gel	1 bottle	$20	$20
FSR Pressure Sensor	1	$3	$3
MPRLS Pressure Sensor	1	$15	$15
Nuts / Screws/ Bolts	NA	NA	$300
B-454 Transducer	1	Provided by Faculty Advisor	$0
Voltage Sensor	1	$10	$10
PS4 Controller	1	$65	$65
Single Channel Relay	1	$7	$7
Transducer Circuit Board	1	$50	$50
Total			$1663

TABLE A.2: Total expected spending for the project based on amount spent to date.

Needed Items	*Quantity*	*Price per Unit*	*Total Price*
Robots	2	$1663	$3326
Research Materials	NA	NA	$300
Shipping Costs	NA	NA	$500
Taxes	4	$16	$500
Total			$4626

TABLE A.3: Electrical components on the robot and the current drawn by each. Arduino and Teensy microcontrollers are connected to the Raspberry Pi 4 and are therefore not included since they do not draw current directly from a power supply.

Components	*Quantity*	*Current per Component (mA)*	*Total Current (mA)*
Raspberry Pi 4	1	3,500	3,500
Time of Flight Sensor	6	10	60
Ultrasonic Sensors	3	15	45
Intel RealSense T265	1	300	300
Pressure Sensors	1	0.003	0.003

Components	*Quantity*	*Current per Component (mA)*	*Total Current (mA)*
Vacuum Pump	1	1,000	1,000
Servo Motors	2	1,200	2,400

TABLE A.4: Tomas 1410-0300 Oil-less Diaphragm Vacuum pump specifications.

Specification	*Value*
Length	83 mm
Width	30 mm
Height	54 mm
Net Weight	0.17 kg
Max Vacuum	-76 kPa

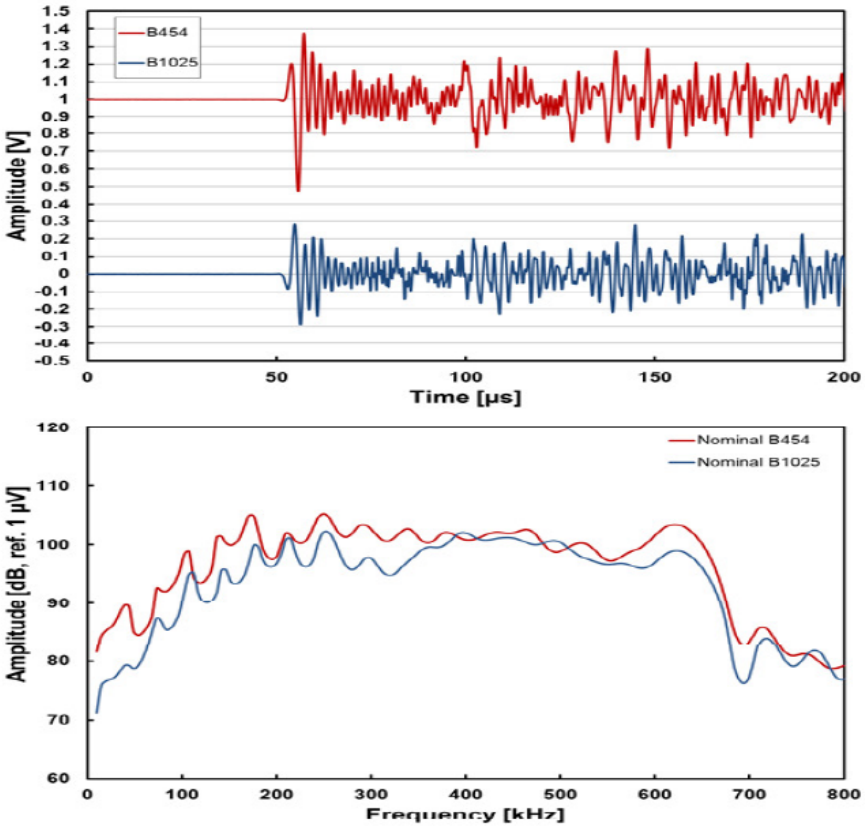

Comparison of B454 and B1025 sensors. Time and Frequency domain responses for a dominant in-plane plate-wave excitation source.

Figure A.5: Amplitude and frequency range for the B454 transducer, compared to an older model. Graphs taken from the datasheet for the B454.